Macro-regenerative nodules in biliary atresia: CT/MRI findings and their pathological relations

Jiun-Lung Liang, Yu-Fan Cheng, Allan M Concejero, Tung-Liang Huang, Tai-Yi Chen, Leo Leung-Chit Tsang, Hsin-You Ou

Jiun-Lung Liang, Yu-Fan Cheng, Tung-Liang Huang, Tai-Yi Chen, Leo Leung-Chit Tsang, Hsin-You Ou, Departments of Diagnostic Radiology, Chang Gung Memorial Hospital-Kaohsiung Medical Center, and Chang Gung University College of Medicine, Kaohsiung 83305, Taiwan, China
Allan M Concejero, Departments of Surgery, Chang Gung Memorial Hospital-Kaohsiung Medical Center, and Chang Gung University College of Medicine, Kaohsiung 83305, Taiwan, China
Author contributions: Liang JL and Chen YF designed the research; Liang JL, Tsang LLC, and Ou HY collected the data; Huang TL and Chen TY interpreted the images; Liang JL wrote the paper; Concejero AM revised the manuscript.
Correspondence to: Dr. Yu-Fan Cheng, Department of Diagnostic Radiology, Chang Gung Memorial Hospital, 123 Tai-Pei Road, Niao-Sung, Kaohsiung 83305, Taiwan, China. cheng.yufan@msa.hinet.net
Telephone: +886-7-7317123-3027 Fax: +886-7-7318762
Received: May 20, 2008   Revised: June 23, 2008
Accepted: June 30, 2008
Published online: July 28, 2008

Abstract

AIM: To describe the radiological findings of a macro-regenerative nodule (MRN) in the liver of pre-transplantation biliary atresia (BA) patients and to correlate it with histological findings.

METHODS: Between August 1990 and November 2007, 144 BA patients underwent liver transplantation (LT) at our institution. The pre-transplantation computer tomography (CT) and magnetic resonance imaging (MRI) findings were reviewed and correlated with the post-transplantation pathological findings.

RESULTS: Nine tumor lesions in 7 patients were diagnosed in explanted livers. The post-transplantation pathological findings showed that all the lesions were MRNs without malignant features. No small nodule was detected by either MRI or CT. Of the 8 detectable lesions, 6 (75%) were in the central part of the liver, 5 (63%) were larger than 5 cm, 5 (63%) had intra-tumor tubular structures, 3 (38%) showed enhancing fibrous septa, 3 (38%) had arterial enhancement in CT, one (13%) showed enhancement in MRI, and one (13%) had internal calcifications.

CONCLUSION: Although varied in radiological appearance, MRN can be differentiated from hepatocellular carcinoma (HCC) in most of BA patients awaiting LT. The presence of an arterial-enhancing nodule does not imply that LT is withheld solely on the basis of presumed malignancy by imaging studies. Liver biopsy may be required in aid of diagnostic imaging to exclude malignancy.

INTRODUCTION

Biliary atresia (BA), the congenital absence or destruction of the intra- or extra-hepatic biliary system[1], affects about 5-10/100 000 live births[2]. Porto-enterostomy is typically performed as soon as possible in these children[3,4]. However, liver cirrhosis and its complications may develop in some patients even after a successful porto-enterostomy. Liver transplantation (LT) is, thus, beneficial to BA, and is the leading reason for LT in children[5].

Macro-regenerative nodule (MRN), defined as a regenerating liver nodule > 0.5 cm in size, is occasionally encountered in cirrhotic livers[6] and may mimic a hepatocellular carcinoma (HCC)[7,8]. Differentiating this benign entity from HCC may be challenging, but is very important when considering patients for LT. Although the clinical importance of MRN in BA patients have been discussed[9], further details of its computer tomography (CT) and magnetic resonance imaging (MRI) radiological appearances remain to be elucidated. The objective of this study was to describe the CT and MRI appearances of MRN in BA patients, and their radiological importance.

MATERIALS AND METHODS

Patients

We reviewed the images, medical records, and pathological reports of 144 BA patients who underwent LT from August 1990 to November 2007 in Chang Gung Memorial Hospital-Kaohsiung Medical Center, Taiwan, China. The diagnosis of BA was proven by surgical and pathological findings after porto-enterostomy in all patients. Of the 144 patients, routine liver CT angiography and MRI were not performed in 33 patients before September 2000 because no standard procedure was available. However, there were no liver masses described in the pathological reports in these 33 patients. A total of 111 patients were included in this study.

CT

Preoperative imaging evaluation was performed in the 111 patients using Somaton plus 4 spiral CT scanner (Siemens, Erlangen, Germany). Sedation using intravenous propofol (0.5-1 mg/kg body weight) without tracheal intubation was given in uncooperative patients. The scanning protocol was 5-mm collimation and a 1:1.5 pitch. The images were subsequently reconstructed at a 4- or 5-mm interval with scanning range from lung base to liver edge. Non-contrast enhanced scanning was performed followed by contrast enhanced scans utilizing an intravenous contrast medium (1.5-2 mL/kg body weight) injected at 1.5 mL/s with an automated power injector via a 22- or 24-gauge intravenous catheter. The arterial phase acquisition started at 20-25 s, porto-venous phase at 60-70 s and equilibrium phase at 3-5 min after intravenous administration of a contrast medium.

MRI

Seventy-nine of the 111 patients underwent MRI examination. We used a 1.5-T superconducting imager (Gyroscan Intera, Philips Medical system, Netherland B.V.) equipped with a phase-array body-coil. The liver was imaged in the axial planes with the following sequences: T1WI (GRE), T2WI (SENSE) and contrast-enhanced T1WI (GR). T1WI (GRE) was conducted using the following parameter: a repetition time/ echo time of 10/4.6 milliseconds. The T2WI (SENSE) was imaged using the following parameter: a repetition time/ echo time of 600/80 milliseconds.

For all the pulse sequences, a 5-8 mm thick slice was used with a 2 mm gap, 256×256 matrix size, echo train length of 1, number of average of 1 and a 35-40 field of view, depending on the size of the individual patient's liver.

A contrast medium was administrated using gadolinium-DTPA (0.1 mmole/kg body weight, Magnevist, Schering, Berlin, Germany) followed by a 20-mL saline flush. The delay for image acquisition timing was determined with a bolus tracking technique. Image reconstruction with 5-8 mm thickness was performed with source images at a MRI workstation.

Image interpretation

Two radiologists experienced in reading abdominal radiography retrospectively reviewed the images from the picture archiving and communicating system (PACS, GE medics) or from the patient's file storage (before 2002). Arterial, porto-venous and equilibrium phase images were interpreted conjointly. Preoperative assessment of the liver nodules included the number, location, size (the largest diameter in 3D orthogonal view), morphology, enhancing pattern, and signal intensity in MRI.

Histopathologic review

All explanted livers were serially sliced at 0.5 cm intervals and carefully inspected to detect the focal lesions seen during preoperative imaging. The size and location of all visible nodules were recorded at gross inspection. All macroscopic nodules were examined microscopically for histological identification and differentiation. Representative sections of the liver were also examined.

Serum alpha-fetoprotein (AFP)

Serum AFP values were determined in all patients at the time of imaging or before transplantation.

RESULTS

Nine MRN were detected in the explanted liver of 7 (4.8%) out of the 111 patients. The mean nodule diameter was 5.9 cm (range 1.6-9 cm). The MRN were located in the medial aspect (hepatic segments 4, 5, and 8) of 6 (67%) patients and in the lateral part of the liver (hepatic segments 2, and 6) of 3 (33%). The margin of the nodules was well-defined in all specimens. Of these 9 MRN, 7 were detected by CT and 7 by MRI. One was not detected by either MRI or CT, and one was found by MRI only. One patient with MRN did not undergo MRI. The CT and MRI findings of the 8 detectable MRN are listed in Table 1. At CT, the MRN were hyperdense compared with the surrounding liver parenchyma before contrast in 6 (75%) nodules (Figure 1A), the other 3 (38%) nodules were isodense (Figure 2A). After contrast medium enhancement, one nodule (13%) showed prominent enhancement both in arterial phase and in porto-venous phase, two nodules (25%) showed early enhancement and early wash-out pattern (Figure 3A), and four (50%) nodules showed no enhancement.

At MRI, the nodule was isointense to hyperintense on T1WI sequences and hypointense in T2WI in 5 (63%) nodules (Figure 1B) with one nodule showing T2WI central hyperintensity. Two nodules (25%) were hypointense on T1WI and hyperintense in T2WI (Figure 2B). After contrast enhancement, only one nodule showed enhancement. The other characteristic radiological findings in CT and MRI included stretching of intratumor tubular structures (5 lesions) (Figures 1C and 3B), fibrous septa in the periphery of the nodules (2 lesions), and internal calcifications (1 lesion). The septa were hypointense both before and after enhancement in T1WI.

Histopathology displayed that all lesions were MRN (Figures 1D and 3C), which were described as well-circumscribed liver cell nodules showing proliferating uniform liver cells bearing uniform round nuclei and
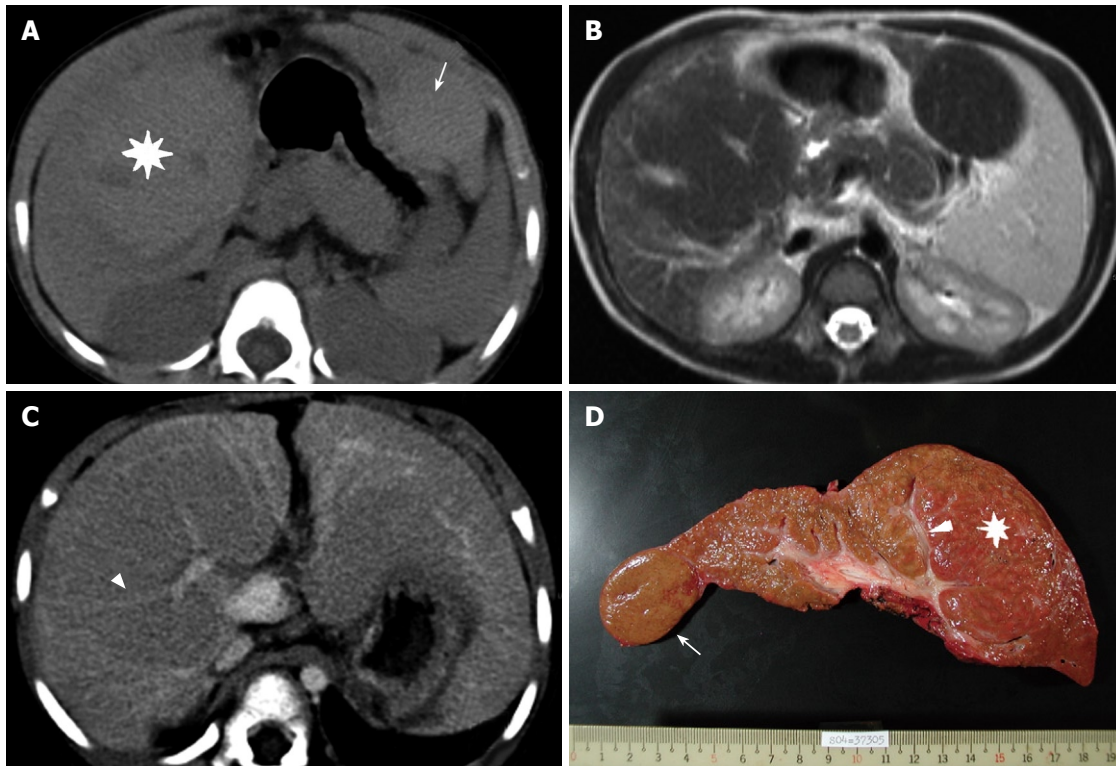
Figure 1 A 3-year-old BA girl with segments 5-8 (asterisk) and segment 2 (arrow) MRN. **A**: The density of the MRN is slightly higher than that in the surrounding liver parenchyma during pre-enhanced phase of the CT; **B**: FSE/T2WI MRI shows a lower signal intensity in the MRN than in the surrounding liver; **C**: During portovenous phase of the CT, the tubular structure and splaying portal veins can be seen in the MRN (arrowhead); **D**: The explanted liver and intra-tumoral portal tract can be seen (arrowhead).

Table 1 Summary of CT and MRI characteristics

	Case 1	Case 2	Case 3	Case 4	Case 5	Case 6	Case 7
Size (cm)	9; 5; 1.6[1]	4.5	2.1	3.5	7	7.5	13
Location (segment)	S5-8/S2	S6	S8	S5	S4-5-8	S4-5-8	S5-6-7-8
Density in CT (-) relative to liver parenchyma	Hyperdense; Hyperdense	Hyperdense	Isodense	Isodense	Hyperdense	Hyperdense	Hyperdense
Enhancement in CT	No	Early enhancement and early wash-out	Delayed portovenous enhancement	No	Arterial and portovenous enhancement	No	Early patchy enhancement early wash-out
MRI T1WI/T2WI/C+	Hyperintense/ Hypointense	Hyperintense/ Hypointense	Hypointense/ Hyperintense	Hypointense/ Hyperintense	Not done	Hyperintense/ Hypointense	Isointense/ Hypointense
Septa T1WI/T2WI/C+	Not discernible	Hypointense/ Hypointense/ Enhanced	Not discernible	Not discernible	Not done	Hypointense/ Hypointense/ Enhanced	Not discernible
Presence of internal tubular structure (portal tract)	Yes; yes	No	No	No	Yes	Yes	Yes
Calcifications	No	No	No	Yes	No	No	No

[1]This small nodule is not detected by either CT or MRI.

eosinophilic cytoplasm. No cellular atypia was found. The liver cells were arranged in one- to two-cell thick plates with intervening sinusoids (Figure 3D). No apparent sinusoidal capillarization was seen in the tumor lesion and no malignant foci were identified. Abortive portal tract formation was also noted. In all the seven MRN patients, the AFP level was < 3 ng/mL before LT.

DISCUSSION

Multi-acinar MRN, first described by Edmondson in 1976[10], are sometimes seen in the cirrhotic liver. In 1996, an International Working Party defined MRN as "at least 5 mm regenerative nodules containing more than one portal tract"[10]. The reported prevalence in autopsy and explanted series varies from 14.2% in nodules > 1 cm in diameter to 37% in nodules > 0.5 cm in diameter[6,11,12]. It has been proposed that nodules > 2 cm in diameter in a background of cirrhosis are almost always dysplastic. However, these data were derived mainly from viral- or alcoholic-related cirrhotic livers. The smallest lesion found at gross pathology in our series was 1.6 cm in
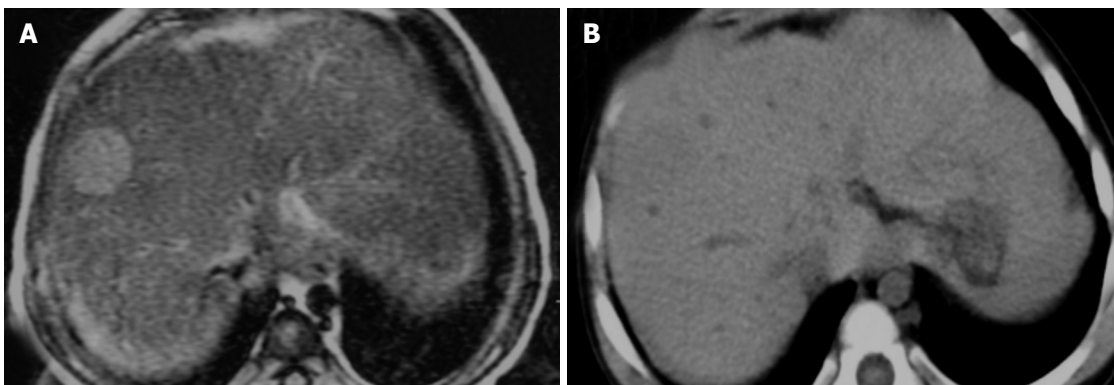
Figure 2 A 16-month-old BA girl with a 2.1 cm MRN in segment 8. **A**: During pre-enhanced phase of the CT, no nodule can be seen; **B**: The signal intensity is hyperinstense on T2WI MRI.
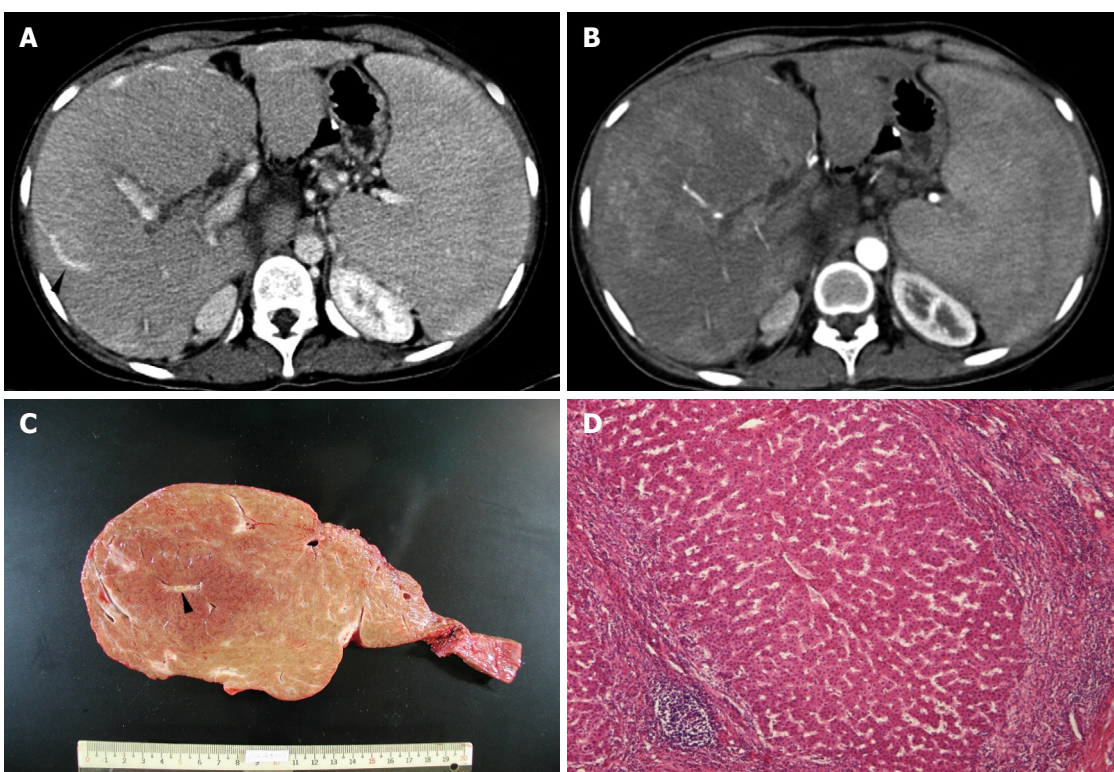

Figure 3 Patchy arterial enhancement within the mass in arterial phase of the CT (**A**), tubular structure (arrowhead) within the mass during portovenous phase of the CT (**B**), the explanted liver and intra-tumoral portal tract (arrowhead) (**C**), and microscopic examination (HE) showing uniform benign-looking liver cells arranged in one- to two-cell thick plates with intervening sinusoids and surrounding fibrous septa infiltrated with lymphocyte (**D**) in a 3-year-old BA girl with 13 cm MRN in right liver.

diameter and 56% (5/9) of the nodules were > 5 cm in diameter (Figure 1A). In the literature, lesions > 10 cm in diameter have been reported[13,14].

MRN can be divided into siderotic and non-siderotic types[15] based on the presence of iron deposition within the mass. The presence of iron results in hypointense signal especially with longer TE MRI pulse sequences[16]. In this study, 63% (5/8) of the regenerating nodules fit this pattern (Figure 1B)[17,18]. In non-siderotic regenerating nodules (2/8), the patterns included T1 hypointensity and T2 hyperintensity (Figure 2B). These non-siderotic MRN are difficult to see on pre-enhanced CT due to their isodensity with the surrounding liver parenchyma (Figure 2A). Because of the retrospective

design of the current study, our methodology did not include histopathologic proof that the decreased signal intensity seen was caused by hepatic iron deposition. However, the same imaging techniques have been used to detect hepatic iron overload and siderotic regenerative nodules, and the results were confirmed with quantitative histopathologic measurements[19-21].

In CT hepatic angiography, MRN have been characterized as non-enhancing nodules surrounded by enhancing fibrous septa[22]. However, in our study, this structural pattern was not easily seen. Only 25% (2/8) in our cases had broad vascular septa partially discernable by MRI. These septa were hypointense on T1W images, perhaps due to the fibrous component of the septum

itself. Enhancing septa were seen only in two nodules in this series after gadolinium-DTPA administration.

Fifty-three percent (5/8) of the MRN in our series had characteristic internal enhancing tubular structures during porto-venous phase. This was particularly true in the larger masses (Figures 1C and 3B). The enhancing tubular structures correlated with a distorted portal vein accompanying a bile duct on histopathology (Figures 1D and 3C). MRN virtually always contain some normal-appearing abortive portal tracts with complete portal veins, hepatic arteries and bile ducts[10]. Importantly, as a regenerative nodule progresses to become a dysplastic nodule or early HCC, one may notice the loss of visualization of these portal tracts and development of new arterial vessels, termed non-triadal arteries. These features are often used to differentiate MRN from adenoma or carcinoma pathologically. Therefore, the imaging appearance of these characteristic findings may be useful in diagnosing MRN during the pretransplant survey among BA patients awaiting LT.

Other useful imaging features used to differentiate MRN from HCC have been described elsewhere. First, a MRN is usually hyperdense to liver parenchyma in pre-enhanced study and often (but not always) does not enhance post contrast. A typical HCC is hypodense or isodense to liver parenchyma in pre-enhanced study and shows early arterial enhancement and early washout in porto-venous phase in dynamic-enhanced CT[23]. Second, the signal intensity of MRN in T2WI is often hypointense while malignant tumors are often hyperintense[23,24]. Third, MRN, especially larger ones, show splaying of intratumor portal veins while malignant tumors usually demonstrate displaced or obliterated portal veins. However, there are some overlapping features between MRN and HCC[25]. In a cirrhotic liver, early reports suggested that virtually all arterial-enhancing lesions are HCC. However, arterial enhancement may be seen in a regenerating nodule, non-tumor arterio-portal shunt, and aberrant venous drainage in a cirrhotic liver[8,26,27]. Our series demonstrated that arterial enhancement also occurred in MRN of BA patients.

A MRN has been presumed to be a precancerous lesion in virus-related or alcoholic-related liver cirrhosis because malignant foci are occasionally found in MRN[28,29]. Although rare, one case report has described a small HCC in a BA-related cirrhotic liver[30]. The possibility of early HCC could not be excluded in some of our pre-transplant imaging surveys of BA patients. According to the non-invasive diagnostic criteria for HCC proposed by the European Association for the Study of the Liver[31,32], a diagnosis of HCC is established by the concomitant positive findings in two imaging techniques, or by a positive findings in one imaging technique with an AFP > 400 μg/L. The radiological interpretations for three arterial-enhancing tumor lesions (patient 2, 5 and 7) in this series were HCC initially (Figure 3A). Using the Barcelona Clinic Liver Cancer staging classification and treatment schedule, LT is considered for patients with three nodules < 3 cm in diameter or with one tumor < 5 cm in diameter and liver function impairment[33]. LT may be precluded in patients 5 and 7 if the HCC diagnosis was made based solely on imaging. Furthermore, the AFP values for all cases were < 3 ng/mL. In such a situation, liver biopsy is necessary to confirm the nature of an arterial enhancing mass in order to exclude hepatic malignancy.

In conclusion, MRN are seen in about 5% of patients with BA awaiting LT. CT and MRI imaging features of MRN as described in this review can be useful in differentiating MRN from HCC in most of BA patients awaiting LT. The presence of an arterial-enhancing nodule should not imply that LT should be withheld solely on the basis of presumed malignancy by imaging studies, especially if the AFP value is incongruent with radiographic findings. Liver biopsy may be required in aid of diagnostic imaging to exclude malignancy in these cases.

COMMENTS

Background
End stage liver cirrhosis develops in some biliary atresia (BA) patients later in life. Liver transplantation (LT) is beneficial to such patients. Macro-regenerative nodules (MRNs) in cirrhotic liver are occasionally encountered in computer tomography (CT) / magnetic resonance imaging (MRI) and may be confused with hepatocellular carcinoma (HCC).

Research frontiers
The authors described typical and atypical CT/MRI appearance of the MRN in BA patients, and the criteria for differentiation of MRNs from MRN. The strategy of managing atypical MRNs is also discussed.

Innovations and breakthroughs
This study showed that the majority of MRNs can be easily differentiated from hepatocellullar carcinoma by CT/MRI and unnecessary liver biopsy can be avoided.

Applications
Using the radiographic features presented in this study will help manage BA patients awaiting LT properly.

Terminology
MRN are defined as regenerative nodules larger than 0.5 cm in diameter in a cirrhotic liver. BA is a congenital absence or destruction of the intra- or extra-hepatic biliary system. It affects about 5-10/100 000 live births and is the leading cause for liver transplant in children especially in the oriental population.

Peer review
The authors described the radiological findings of MRN in the liver of pre-transplantation BA patients and correlated it with histological findings. This is an interesting paper, which is informative to readers.

REFERENCES

1   **Sokol RJ**, Mack C. Etiopathogenesis of biliary atresia. *Semin Liver Dis* 2001; **21**: 517-524
2   **Yoon PW**, Bresee JS, Olney RS, James LM, Khoury MJ. Epidemiology of biliary atresia: a population-based study. *Pediatrics* 1997; **99**: 376-382
3   **Hung PY**, Chen CC, Chen WJ, Lai HS, Hsu WM, Lee PH, Ho MC, Chen TH, Ni YH, Chen HL, Hsu HY, Chang MH. Long-term prognosis of patients with biliary atresia: a 25 year summary. *J Pediatr Gastroenterol Nutr* 2006; **42**: 190-195
4   **Sokol RJ**, Mack C, Narkewicz MR, Karrer FM. Pathogenesis and outcome of biliary atresia: current concepts. *J Pediatr Gastroenterol Nutr* 2003; **37**: 4-21
5   **Goss JA**, Shackleton CR, McDiarmid SV, Maggard M, Swenson K, Seu P, Vargas J, Martin M, Ament M, Brill J, Harrison R, Busuttil RW. Long-term results of pediatric liver transplantation: an analysis of 569 transplants. *Ann*

Surg 1998; **228**: 411-420

6   **Furuya K**, Nakamura M, Yamamoto Y, Togei K, Otsuka H. Macroregenerative nodule of the liver. A clinicopathologic study of 345 autopsy cases of chronic liver disease. *Cancer* 1988; **61**: 99-105

7   **Farrell R**, Steinman A, Green WH. Arteriovenous shunting in a regenerating liver simulating hepatoma. Report of a case. *Radiology* 1972; **102**: 279-280

8   **Brancatelli G**, Baron RL, Peterson MS, Marsh W. Helical CT screening for hepatocellular carcinoma in patients with cirrhosis: frequency and causes of false-positive interpretation. *AJR Am J Roentgenol* 2003; **180**: 1007-1014

9   **Liu YW**, Concejero AM, Chen CL, Cheng YF, Eng HL, Huang TL, Chen TY, Wang CC, Wang SH, Lin CC, Yong CC, Yang CH, Jordan AP, Jawan B. Hepatic pseudotumor in long-standing biliary atresia patients undergoing liver transplantation. *Liver Transpl* 2007; **13**: 1545-1551

10   **Terminology of nodular hepatocellular lesions.** International Working Party. *Hepatology* 1995; **22**: 983-993

11   **Le Bail B**, Belleannee G, Bernard PH, Saric J, Balabaud C, Bioulac-Sage P. Adenomatous hyperplasia in cirrhotic livers: histological evaluation, cellular density, and proliferative activity of 35 macronodular lesions in the cirrhotic explants of 10 adult French patients. *Hum Pathol* 1995; **26**: 897-906

12   **Terada T**, Terasaki S, Nakanuma Y. A clinicopathologic study of adenomatous hyperplasia of the liver in 209 consecutive cirrhotic livers examined by autopsy. *Cancer* 1993; **72**: 1551-1556

13   **Wang ZJ**, Coakley FV, Ferrell LD, Rosenthal P. CT and MRI of hepatic pseudotumor in long-standing biliary atresia. *J Comput Assist Tomogr* 2002; **26**: 444-447

14   **Gurkan A**, Sherlock MF, Chui AK, Thomson R, Verran D, Sheil AG, Painter D. A giant multiacinar macroregenerative nodule in an explanted liver. *Transplantation* 2001; **72**: 538-539

15   **Terada T**, Nakanuma Y. Survey of iron-accumulative macroregenerative nodules in cirrhotic livers. *Hepatology* 1989; **10**: 851-854

16   **Krinsky GA**, Lee VS, Theise ND, Weinreb JC, Rofsky NM, Diflo T, Teperman LW. Hepatocellular carcinoma and dysplastic nodules in patients with cirrhosis: prospective diagnosis with MR imaging and explantation correlation. *Radiology* 2001; **219**: 445-454

17   **Ohtomo K**, Itai Y, Ohtomo Y, Shiga J, Iio M. Regenerating nodules of liver cirrhosis: MR imaging with pathologic correlation. *AJR Am J Roentgenol* 1990; **154**: 505-507

18   **Murakami T**, Nakamura H, Hori S, Nakanishi K, Mitani T, Tsuda K, Kozuka T, Wakasa K, Monden M. CT and MRI of siderotic regenerating nodules in hepatic cirrhosis. *J Comput Assist Tomogr* 1992; **16**: 578-582

19   **Ernst O**, Sergent G, Bonvarlet P, Canva-Delcambre V, Paris JC, L'Hermine C. Hepatic iron overload: diagnosis and quantification with MR imaging. *AJR Am J Roentgenol* 1997; **168**: 1205-1208

20   **Gandon Y**, Guyader D, Heautot JF, Reda MI, Yaouanq J, Buhe T, Brissot P, Carsin M, Deugnier Y. Hemochromatosis: diagnosis and quantification of liver iron with gradient-echo MR imaging. *Radiology* 1994; **193**: 533-538

21   **Ito K**, Mitchell DG, Gabata T, Hann HW, Kim PN, Fujita T, Awaya H, Honjo K, Matsunaga N. Hepatocellular carcinoma: association with increased iron deposition in the cirrhotic liver at MR imaging. *Radiology* 1999; **212**: 235-240

22   **Murakami T**, Kuroda C, Marukawa T, Harada K, Wakasa K, Sakurai M, Monden M, Kasahara A, Kawata S, Kozuka T. Regenerating nodules in hepatic cirrhosis: MR findings with pathologic correlation. *AJR Am J Roentgenol* 1990; **155**: 1227-1231

23   **Taylor AJ**, Carmody TJ, Quiroz FA, Erickson SJ, Varma RR, Komorowski RA, Foley WD. Focal masses in cirrhotic liver: CT and MR imaging features. *AJR Am J Roentgenol* 1994; **163**: 857-862

24   **Matsui O**, Kadoya M, Kameyama T, Yoshikawa J, Arai K, Gabata T, Takashima T, Nakanuma Y, Terada T, Ida M. Adenomatous hyperplastic nodules in the cirrhotic liver: differentiation from hepatocellular carcinoma with MR imaging. *Radiology* 1989; **173**: 123-126

25   **Nagasue N**, Yukaya H, Chang YC, Kimura N, Ota N, Nakamura T. Hepatocellular pseudotumour (regenerating nodule) in the cirrhotic liver mimicking hepatocellular carcinoma. *Br J Surg* 1988; **75**: 1124-1128

26   **Dodd GD 3rd**, Baron RL, Oliver JH 3rd, Federle MP. Spectrum of imaging findings of the liver in end-stage cirrhosis: Part II, focal abnormalities. *AJR Am J Roentgenol* 1999; **173**: 1185-1192

27   **Kim TK**, Choi BI, Han JK, Chung JW, Park JH, Han MC. Nontumorous arterioportal shunt mimicking hypervascular tumor in cirrhotic liver: two-phase spiral CT findings. *Radiology* 1998; **208**: 597-603

28   **Takayama T**, Makuuchi M, Hirohashi S, Sakamoto M, Okazaki N, Takayasu K, Kosuge T, Motoo Y, Yamazaki S, Hasegawa H. Malignant transformation of adenomatous hyperplasia to hepatocellular carcinoma. *Lancet* 1990; **336**: 1150-1153

29   **Nakanuma Y**, Terada T, Ueda K, Terasaki S, Nonomura A, Matsui O. Adenomatous hyperplasia of the liver as a precancerous lesion. *Liver* 1993; **13**: 1-9

30   **Brunati A**, Feruzi Z, Sokal E, Smets F, Fervaille C, Gosseye S, Clapuyt P, de Ville de Goyet J, Reding R. Early occurrence of hepatocellular carcinoma in biliary atresia treated by liver transplantation. *Pediatr Transplant* 2007; **11**: 117-119

31   **Bruix J**, Sherman M, Llovet JM, Beaugrand M, Lencioni R, Burroughs AK, Christensen E, Pagliaro L, Colombo M, Rodes J. Clinical management of hepatocellular carcinoma. Conclusions of the Barcelona-2000 EASL conference. European Association for the Study of the Liver. *J Hepatol* 2001; **35**: 421-430

32   **Llovet JM**, Burroughs A, Bruix J. Hepatocellular carcinoma. *Lancet* 2003; **362**: 1907-1917

33   **Llovet JM**, Bru C, Bruix J. Prognosis of hepatocellular carcinoma: the BCLC staging classification. *Semin Liver Dis* 1999; **19**: 329-338